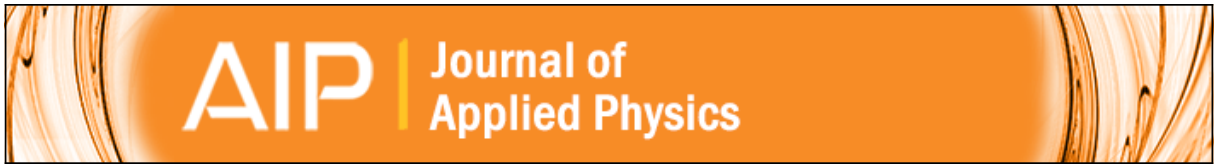

Structural modifications in Fe x Co 1 x Cu multilayers induced by ion irradiation

I. L. Graff, S. R. Teixeira, L. Amaral, M. C. Martins Alves, and W. H. Flores

Citation: Journal of Applied Physics **96**, 1469 (2004); doi: 10.1063/1.1767288
View online: http://dx.doi.org/10.1063/1.1767288
View Table of Contents: http://scitation.aip.org/content/aip/journal/jap/96/3?ver=pdfcov
Published by the AIP Publishing

[This article is copyrighted as indicated in the article. Reuse of AIP content is subject to the terms at: http://scitation.aip.org/termsconditions. Downloaded to] IP: 200.130.19.173 On: Fri, 21 Mar 2014 17:27:31

HTML ABSTRACT + LINKS

Structural modifications in Fe_xCo_{1-x}/Cu multilayers induced by ion irradiation

I. L. Graff, S. R. Teixeira, L. Amaral,[a] and M. C. Martins Alves
Instituto de Física—UFRGS, Caixa Postal 15051, 91501-970 Porto Alegre, Brazil

W. H. Flores
Departamento de Física—UFC, Caixa Postal 6030, 60455-760 Fortaleza, Brazil

(Received 3 October 2003; accepted 6 May 2004)

The structural evolution of $Fe_{30}Co_{70}$/Cu multilayers under ion irradiation is investigated in detail using x-ray techniques. The samples were irradiated with two different ions, 50 keV of He^+ and 600 keV of Kr^+, at room temperature. No substantial changes were observed after He^+ irradiation; the He^+ ions promote some disorder in the FeCo layers, an increase of the Cu(111) texture, and grain size. After Kr^+ irradiation a structural phase transition from bcc to fcc occurs in the FeCo layers. A very pronounced increase of the Cu(111) texture and grain size is also observed. According to the equilibrium phase diagrams such fcc phase is not expected for the FeCo alloy at the composition of $Fe_{30}Co_{70}$. This fcc phase is imposed by the Cu fcc structure of the adjacent layers, which induce the regrowth of the FeCo layers structure from bcc to fcc during the relaxation period of the atomic collision cascades. Also, after the Kr^+ irradiation a multilayer structure still persists, as showed by the x-ray reflectivity. © *2004 American Institute of Physics*.
[DOI: 10.1063/1.1767288]

I. INTRODUCTION

Ion irradiation of multilayers has been used for a long time as a technique to induce structural changes in a variety of materials. These materials under ion irradiation undergo significant atomic rearrangement. An example of this phenomenon is the atomic intermixing and alloying that can occur at the interface separating two different materials during ion irradiation.[1] Ion-beam mixing can produce modified materials, with higher solute concentrations at lower irradiation doses than can be achieved with conventional high-dose implantation techniques. It is well known that an energetic ion beam may induce alloying as it passes through the interface that separates two different materials. Moreover, ion irradiation of crystalline metallic alloys causes structural changes, and crystalline phases can become amorphous or change to a different crystalline structure.[2,3]

Another application of ion irradiation emerged recently. It was used as a nanometer scale technique for magnetic media patterning, with possibility of controlling magnetization reversal properties and medium planarity, two fundamental aspects in the new magnetic recording technology.[4] Chappert *et al.*[5] used ion irradiation to fabricate magnetic patterned films irradiating it through a mask to create local modifications on the film properties. In this case, localized modifications of magnetic coercivity and easy-magnetization axis, in Co/Pt multilayers, were obtained with 30 keV He^+ ions. The influence on the magnetic properties of Ni/Fe films after ion irradiation has also been reported[6,7] as much as other magnetic systems such as Co/Ag, which were studied in detail by structural evolution and magnetic response.[8,9]

The Fe_xCo_{1-x}/Cu multilayer system is of great interest from both fundamental and applied points of view because this multilayered system as well as FeCo-Cu granular films can present large values of giant magnetoresistance.[10,11] In particular, systems with $Fe_{30}Co_{70}$/Cu alloy compositions exhibited one of the largest magnetoresistance amplitude reported so far at 4 K in granular alloys.[12,13] Nowadays, Fe_xCo_{1-x} systems are also used in magnetic tunnel junctions with spin-valve architecture such as magnetic tunnel transistor devices.[14]

In order to understand the magnetic behavior of the $Fe_{30}Co_{70}$/Cu multilayers under ion irradiation it is necessary first to investigate the structural evolution. We are mainly concerned with the structural modifications induced by room temperature ion irradiation of the $Fe_{30}Co_{70}$/Cu multilayers. The irradiations were performed with two different ions, He^+ and Kr^+. The experiment reported here was developed to study the structural modifications in the $Fe_{30}Co_{70}$/Cu multilayers after ion irradiation by means of x-ray techniques, namely, x-ray diffraction, x-ray reflectivity, and x-ray absorption spectroscopy.

II. EXPERIMENTAL METHODS

The $[Fe_{30}Co_{70}(15\ Å)/Cu(50\ Å)]_{\times 10}$ multilayers were prepared by alternate electron-beam evaporation of Cu and $Fe_{30}Co_{70}$ alloy at 3×10^{-8} mbar on a commercial oxidized Si(111) substrate. To avoid any oxidation of the FeCo alloy, a cap layer of 30 Å of Cu was deposited over the last layer of FeCo. The evaporation was done at room temperature in a BALZERS UMS-500P system using a 1 Å/s deposition rate monitored by a computer controlled quartz microbalance. The ion irradiations at room temperature were carried out in a 500 keV ion implanter. For our purposes, the samples were

[a]Author whom correspondence should be addressed; electronic mail: amaral@if.ufrgs.br

 © 2004 American Institute of Physics

[This article is copyrighted as indicated in the article. Reuse of AIP content is subject to the terms at: http://scitation.aip.org/termsconditions. Downloaded to] IP: 200.130.19.173 On: Fri, 21 Mar 2014 17:27:31

irradiated with 50 keV of He^+ (1×10^{17} ions/cm^2) and 600 keV of Kr^+ (3×10^{15} ions/cm^2) with current densities of 1 μA/cm^2 and 0.1 μA/cm^2, respectively. Energies and doses were calculated using the TRIM code[15] and chosen in such a way that the ions had traversed the whole multilayer thickness and stopped at the substrate, depositing approximately the same total energy in the multilayer stack for both irradiations.

The structural characterization of the samples was made using x-ray reflectivity, x-ray diffraction (XRD), and x-ray absorption spectroscopy (XAS). Reflectivity experiment was performed in a Philips X'Pert MRD diffractometer equipped with a thin film attachment and a long soller collimator to achieve a better resolution. X-ray diffraction patterns were obtained from a Siemens D500 diffractometer with a Bragg-Brentano geometry. Both reflectivity and diffraction were performed using a Cu $K\alpha$ radiation source. In the XAS measurements, x-ray absorption near edge (XANES) and extended x-ray absorption fine structure (EXAFS) spectra were acquired at the Co, Fe, and Cu *K*–edges using the XAS beam line facility at the Laboratório Nacional de Luz Síncrotron (LNLS).[16] The reference spectra of the Cu (fcc), Fe (bcc), and Co (hcp) standard foils were also measured for comparison and data analysis purposes. The spectra of the samples were measured in fluorescence mode using a Si(Li) detector, with the x-ray beam polarization vector in the plane of the samples. The standard foils were measured in transmission mode. The EXAFS spectra were analyzed by standard procedures, using the WINXAS software package.[17] The various neighboring shells were extracted from the EXAFS signals, $\chi(k)$, by Fourier transformation (FT), weighted by k^l in the wave-vector space ranging from 3.0 to 12.0 Å^{-1}, using a standard Hanning window.[18] Structural parameters were obtained from least-squares fitting in *k* space using experimental phase shift and amplitude.

III. RESULTS

A. X-ray diffraction

In Fig. 1 the x-ray diffraction patterns are shown for the as-deposited, irradiated, and postirradiation annealed samples. Also, the x-ray reflectivity curves corresponding to the as-deposited and irradiated samples are shown as an inset in the figure. For the as-deposited sample the reflection corresponding to fcc Cu(111) is visible exhibiting a large full width at half maximum (FWHM), indicating high structural disorder and a small grain size. At right side of the Cu(111) reflection there is a shoulder due to the bcc FeCo(110) reflection; the arrows indicate the expected peak location. This feature is difficult to observe due to three factors: the high structural disorder in both layers FeCo and Cu [see the large FWHM of Cu(111) peak], the proximity of the fcc Cu(111) and bcc FeCo(110) peaks, and the tendency of preferred orientation in the ⟨111⟩ direction for fcc and ⟨110⟩ for bcc during the film growth. The (111) fcc planes are more close packed than (110) bcc planes. Moreover, the Cu layer thickness is much larger than the FeCo, therefore the Cu(111) reflection is much more visible than the FeCo(110) reflection. After He^+ irradiation the grain size and crystallinity

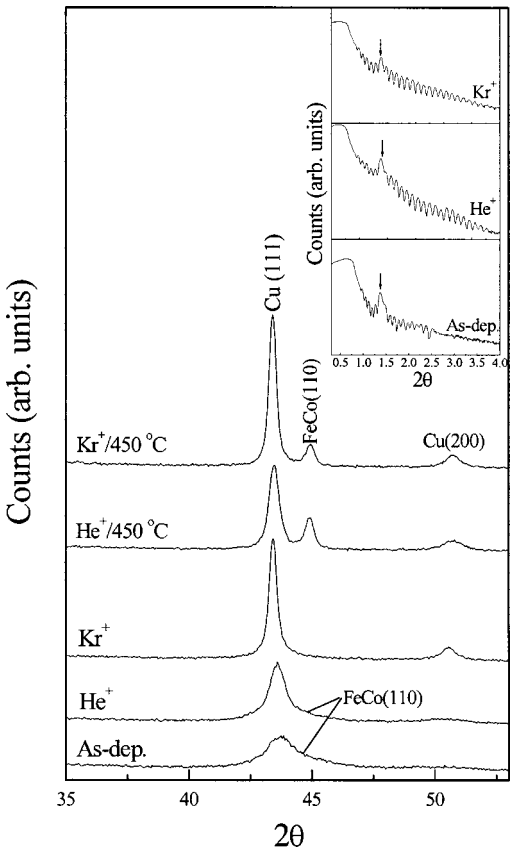

FIG. 1. X-ray diffraction patterns of the as-deposited, irradiated, and postirradiation annealed samples. The x-ray reflectivity curves for the as-deposited and irradiated samples are presented in the inset.

enhances, characterized by the increase of intensity and decrease of FWHM of the Cu(111) peak. At this time, a small waving appears around 50° corresponding to the (200) Cu reflection.

The Kr^+ irradiation also enhances the crystallinity and promotes grain growth. The peak corresponding to the Cu(200) reflection becomes more visible. The shoulder or peak asymmetry that appeared on the right side of Cu(111) peak after He^+ irradiation disappears completely after Kr^+ irradiation. This may be due to a smearing effect produced by the high intensity from the Cu(111) peak or represents an indication of a possible phase transformation of the FeCo alloy layers. Another effect that is observed from the diffraction patterns is the displacement of the Cu(111) peak towards lower values after irradiation. The irradiation triggers a strain release in the multilayers similarly as observed by Devolder[19] in the Co/Pt system after He^+ irradiation. Using a Lorentz profile function[20] to fit this peak we obtained a set of values (lattice parameter *a* and interplanar spacing *d*) that confirm the Cu tensile strain relaxation. The results obtained from this fitting are presented in Table I.

Figure 1 also shows the x-ray reflectivity curves (as an inset) for the as-deposited and irradiated samples. In the figure, the Bragg peaks from the multilayer stack[21] are marked with arrows. After He^+ irradiation the multilayer structure remains, which is confirmed by the presence of the Bragg peak assigned in the figure. This may be explained by the low mixing efficiency of the He^+ ions and the positive heat

[This article is copyrighted as indicated in the article. Reuse of AIP content is subject to the terms at: http://scitation.aip.org/termsconditions. Downloaded to] IP: 200.130.19.173 On: Fri, 21 Mar 2014 17:27:31

TABLE I. Results from the fitting procedure with a Lorentz profile function of the Cu(111) peak. The values for a standard bulk Cu* sample are also shown for comparison.

	As-deposited	He^+	Kr^+	Cu*(111)
2θ (deg)	43.784±0.01	43.605±0.003	43.427±0.001	43.295
d (Å)	2.066	2.074	2.082	2.088
a (Å)	3.578	3.592	3.606	3.615

of mixing[22] ($\Delta H_{mix} > 0$) of the atomic species involved in the multilayer. After Kr^+ irradiation the Bragg peak amplitude decreases, but the peak persists. This shows that almost no mixing occurs, i.e., some kind of multilayer structure is preserved after the Kr^+ irradiation, which is basically an effect of the positive heat of mixing. The diffraction patterns corresponding to the postirradiation annealing, 450°C during 10 min, exhibit clearly the peak from the $Fe_{30}Co_{70}$/Cu alloy. The annealing induces an enhancement of crystallinity in the FeCo alloy and Cu. This figure also shows that if any phase transformation occurs, after Kr^+ irradiation, it is metastable because an annealing with a relatively low temperature of 450°C, during 10 min, destroys this new phase recovering the bcc structure of the FeCo alloy.

B. X-ray absorption spectroscopy

XANES features are fingerprints of the crystallographic structures. So in order to evidence the phase transformation induced by the Kr^+ irradiation we have compared the XANES spectra of the different samples with the ones of Cu (fcc), Fe (bcc), and Co (hcp) references.

Figure 2 shows the Cu *K*-edge XANES spectra of the as-deposited and irradiated samples in comparison with the one of Cu reference. The spectrum of the as-deposited sample is characteristic of a fcc structure. The smoothing of the oscillations corresponds to a high structural disorder present in the film in comparison to the Cu foil, due to the film growth process.

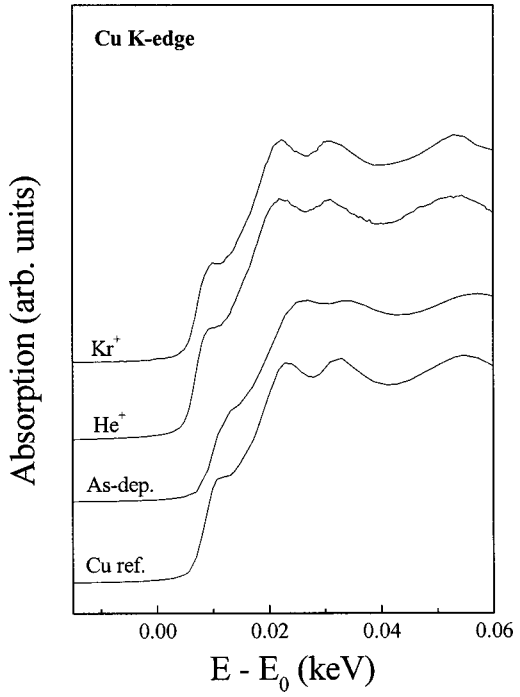

FIG. 2. Cu *K*-edge XANES spectra for the as-deposited and irradiated samples. The Cu reference spectrum is also shown for comparison. The E_0 value corresponds to 8.979 keV.

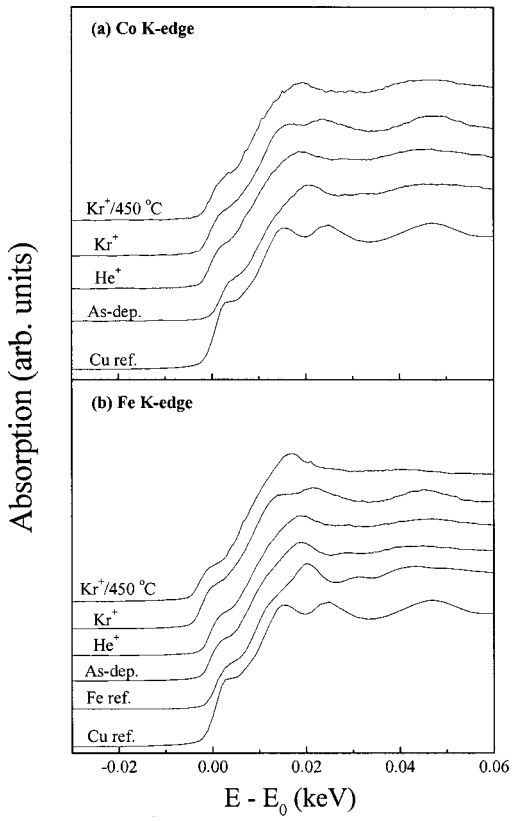

FIG. 3. Co (a) and Fe *K*–edges (b) XANES spectra for the as-deposited, irradiated, and postirradiation annealed samples. The Co, Cu, and Fe reference spectra are shown for comparison. For Co the E_0 value corresponds to 7.709 keV and for Fe to 7.112 keV.

After He^+ and Kr^+ irradiation the fcc structure is kept but with enhancement of crystallinity, the XANES features are much more defined than in the as-deposited sample. Hence, the irradiation improves the crystallinity around Cu in the samples in agreement with the x-ray diffraction patterns.

The XANES spectra at the Co and Fe *K*-edges are displayed in Figs. 3(a) and 3(b), respectively. For the as-deposited sample the XANES features at the Co *K*–edge are characteristic of a bcc structure, as expected for the $Fe_{30}Co_{70}$ alloy in a multilayer stack.[23]

After He^+ irradiation the structure of Co remains bcc with higher structural disorder than the as-deposited sample. Nevertheless, the irradiation with Kr^+ induces considerable changes in the XANES features. The Co assumes fcc structure indicating the occurrence of a phase transition.

When the Kr^+ irradiated sample is annealed at 450°C during 10 min it recovers the primary bcc structure, demonstrating that the fcc phase assumed after Kr^+ irradiation is metastable.

At the Fe *K*–edge [Fig. 3(b)] one observes that Fe assumes the bcc structure in the as-deposited sample. The He^+ irradiation induces some structural disorder but the bcc characteristic is still preserved in the alloy. After Kr^+ irradiation

[This article is copyrighted as indicated in the article. Reuse of AIP content is subject to the terms at: http://scitation.aip.org/termsconditions. Downloaded to] IP: 200.130.19.173 On: Fri, 21 Mar 2014 17:27:31

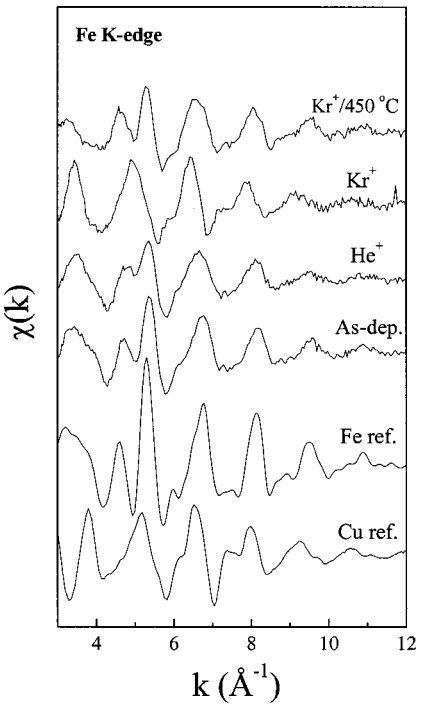

FIG. 4. EXAFS signals for the as-deposited, irradiated, and postirradiation annealed samples at Fe *K*–edge. The Fe and Cu reference signals are also shown for comparison.

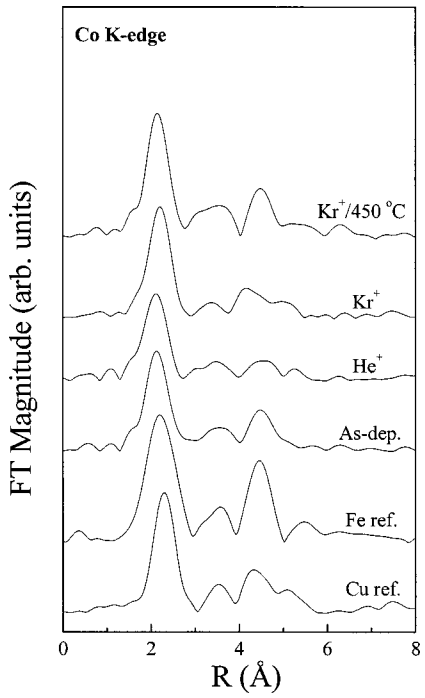

FIG. 5. Co *K*-edge Fourier transforms for the as-deposited, irradiated, and postirradiation annealed samples of the EXAFS signals shown in Fig. 4. The Fe and Cu reference spectra are also shown for comparison.

the structure around Fe is fcc. For the 450 °C annealed sample the contribution of a surface oxide is observed leading to some changes in the XANES spectra. The major changes are the decrease of intensity of the preedge at 0.0 keV, increase of the structure at 0.017 keV, and the damping of the other oscillations.

From the qualitative analysis of the XANES spectra we conclude that the He^+ irradiation only induces structural disorder. In the case of Kr^+ irradiation a phase transformation occurs in the multilayer around the Co and Fe atoms. The FeCo alloy structure changes from bcc, in the as-deposited samples, to fcc after Kr^+ irradiation. According to the equilibrium phase diagram the FeCo at the referred concentration should have a bcc structure.[24] Such conclusion was also observed in a recent investigation about electrodeposited FeCo alloys.[25] This ion-beam-induced fcc phase is not expected so far for this alloy at the present concentration ($Fe_{30}Co_{70}$).

Complementary data that yield quantitative information were obtained from the EXAFS measurements. The EXAFS signals for the as-deposited, irradiated, and postirradiation annealed samples at the Fe *K*–edge are displayed in Fig. 4. As observed previously with the XANES analysis, the as-deposited multilayer displays bcc structure with some structural disorder for the Fe atoms arrangement. After He^+ irradiation the bcc structure is preserved, but after Kr^+ irradiation the structure around the Fe atoms goes to fcc. The EXAFS signals at the Co K–edge show the same trend observed in Fig. 4 and are not presented here. The EXAFS signals, at the Co and the Fe *K*–edges, also show that the fcc phase formed is metastable, turning back to the bcc structure after the 450 °C annealing. The Cu *K*-edge measurements were not shown because the Cu structural environment was almost not affected by the irradiations.

The Fourier transform magnitudes at the Co *K*–edge for the as-deposited, irradiated, and postirradiation annealed samples as well as the standard references (weighted by k^l) are shown in Fig. 5. The FT of the as-deposited sample displays the bcc pattern with some disorder demonstrated by the lower amplitude of the peaks in comparison with the standard reference. Each peak of the FT is related to neighboring shells, where the amplitude depends on the number of atoms in the shell and the position of the peak refers to the distance from the absorbing atom. In the case of a bcc structure, the first peak contains the contribution of two distinct shells, the first and the second one. After He^+ irradiation the position of the FT does not change significantly, but the effect of disorder is more pronounced. After Kr^+ irradiation the FT changes and becomes very similar to the one of Cu reference indicating that the Co environment becomes fcc. The FT of the sample annealed at 450 °C after Kr^+ irradiation displays the bcc pattern showing that the fcc phase is metastable.

The same effect observed around Co (phase transition after Kr^+ irradiation) is also observed around the Fe environment. The FT for the Cu *K*–edge is not shown because the irradiations only enhance the crystallinity of the Cu (fcc) structure as observed from the XANES spectra (Fig. 3).

The results of the quantitative analysis of the first peak of the FT are displayed in Table II. The fit quality is given by ξ^2 (minimized parameter in the fit), which is defined as follows, where N is the number of data points, Δ an estimate for the experimental error, and $y_{\text{expt.}}$ and y_{theor} the experimental and theoretical data points, respectively:

[This article is copyrighted as indicated in the article. Reuse of AIP content is subject to the terms at: http://scitation.aip.org/termsconditions. Downloaded to] IP: 200.130.19.173 On: Fri, 21 Mar 2014 17:27:31

TABLE II. Parameters obtained from the fitting procedure. N_1 and N_2 values correspond to the number of neighbors of the first and second atomic shells. R_1 and R_2 correspond to the mean distance from the absorbing atom to the respective atomic shells, with each Debye-Waller factor (σ_1 and σ_2).

Sample	*K*–edge	$N_1(\pm)$ / $N_2(\pm)$	R_1 (Å)$(\pm)$ / R_2 (Å)$(\pm)$	σ_1^2 (Å^2) / σ_2^2 (Å^2)	ξ^2
As-deposited	Co	8.0 (0.5)	2.46 (0.004)	0.0002	3.9
		5.9 (1.3)	2.88 (0.020)	0.0114	
He^+	Co	6.0 (0.4)	2.48 (0.004)	0.0015	3.5
		6.0 (0.7)	2.72 (0.011)	0.0325	
Kr^+	Co	9.8 (0.1)	2.54 (0.001)	0.0015	2.2
As-deposited	Fe	8.0 (0.6)	2.46 (0.004)	0.0008	0.7
		5.2 (1.1)	2.86 (0.016)	0.0062	
He^+	Fe	8.0 (0.5)	2.47 (0.003)	0.0018	1.4
		5.9 (1.7)	2.86 (0.028)	0.0187	
Kr^+	Fe	9.8 (0.1)	2.54 (0.001)	0.0022	2.0
As deposited	Cu	9.3 (0.1)	2.52 (0.001)	0.0002	1.7
He^+	Cu	11.7 (0.1)	2.52 (0.001)	0.0001	2.7
Kr^+	Cu	12.0 (0.0)	2.53 (0.001)	0.0005	0.9
Co reference	Co	12	2.50		
Fe reference	Fe	8	2.48		
		6	2.86		
Cu reference	Cu	12	2.55		

$$\xi^2 = \frac{1}{\Delta^2}\sum_{i=1}^{N}[y_{\text{expt}}(i) - y_{\text{theor}}(i)]^2.$$

In fitting the EXAFS data, we have always taken into account the information given by the XANES spectra. So, for all the cases that the bcc structure was identified a two-shell fitting was performed.

As can be verified from Table II, the Co environment for the as-deposited and He^+ irradiated samples presents the coordination numbers and distances that correspond to a bcc structure. The He^+ irradiation induces some structural disorder as demonstrated by the increase of the Debye-Waller factor values.

Otherwise, after Kr^+ irradiation the coordination number and distance remain within the uncertainty of the values for a fcc structure. In the case of Fe the same trend is observed.

Around the Cu environment (Cu *K*–edge) both irradiations enhance the crystallinity; the coordination number and distance are within the uncertainty of the bulk values expected for Cu.

IV. DISCUSSION

The fcc phase obtained after Kr^+ ion irradiation is not predicted in the equilibrium phase diagrams of the FeCo alloy at the particular composition ($Fe_{30}Co_{70}$). For this composition a stable bcc phase is expected. Such phase transition happens because the very massive and energetic Kr^+ ions induce a large number of atomic collision cascades when they traverse the multilayer. Such collision cascades will overlap, and as a consequence, a large number of atoms are put in motion through the far-from-equilibrium ion-beam mixing process. After this first step, the highly energetic mixture of atoms will relax toward equilibrium in a second step which takes place in a very short period of time ($10^{-10}-10^{-9}$ s). During this short interval of time the structure of the new formed phase, which will be fixed in the second step, is avoided to undergo directly to an equilibrium state, i.e., the bcc structure. Instead, during this period the Cu layers will impose a fcc structure to the FeCo layers.

In the case of He^+ ion irradiation, there is no phase transformation because the mixing efficiency of these ions is very small. The mass of the incident ion affects the atomic collision cascade development; if the mass is large, as in the case of Kr, the displaced atoms can form a dense continuous region of displaced atoms around the ion track; if the ion mass is small, as in the case of He, small isolated regions of displaced atoms are formed along the ion path. Even with a high dose, there is no complete overlap of the collision cascades in the case of He^+ irradiation, avoiding the formation of a uniformly disordered layer in the whole multilayer to induce the regrowth of the FeCo structure.

V. CONCLUSIONS

We have investigated the structural evolution of $Fe_{30}Co_{70}$/Cu multilayers after He^+ and Kr^+ ion irradiation. The He^+ irradiation induces small changes on the crystalline structure of the multilayer, it produces some structural disorder on the FeCo structure and enhances the Cu(111) texture. After Kr^+ irradiation a phase transition from bcc to fcc is observed in the FeCo alloy layers. A huge increase of Cu(111) texture as well as grain size is also observed. The fcc phase induced by the Kr^+ irradiation is metastable because the bcc structure is regenerated after an annealing during 10 min at 450 °C.

At last, it is interesting to point out that even after He^+ and Kr^+ irradiation a multilayer structure persists. Consequently, ion irradiation of multilayer systems appears to be an efficient method to induce phase transformations in only one set of layers keeping the multilayer structure intact.

ACKNOWLEDGMENTS

This work was financially supported by Brazilian scientific agencies CNPq, FINEP, and FAPERGS. We are very grateful to Dr. Agnès Traverse from Université Paris-Sud (LURE) for the fruitful discussions about ion irradiation and to LNLS staff for their help during the measurements at XAS beam line.

[1] M. Nastasi and J. W. Mayer, Mater. Sci. Eng. Reports R12, 1 (1994).
[2] A. Paesano, Jr., S. R. Teixeira, and L. Amaral, J. Appl. Phys. **70**, 4870 (1991).
[3] B. X. Liu, W. S. Lai, and Q. Zhang, Matter. Sci. Eng. Reports 29, 1 (2000).
[4] E. Betzig, J. K. Trautman, R. Wolfe, E. M. Gyorgy, P. L. Finn, M. K. Kryder, and C.-H. Chang, Appl. Phys. Lett. **61**, 142 (1992).
[5] C. Chappert *et al.*, Science **280**, 1919 (1998).
[6] T. Veres, M. Cai, R. W. Cochrane, M. Rouabhi, S. Roorda, and P. Desjardins, Thin Solid Films **382**, 172 (2001).

[This article is copyrighted as indicated in the article. Reuse of AIP content is subject to the terms at: http://scitation.aip.org/termsconditions. Downloaded to] IP: 200.130.19.173 On: Fri, 21 Mar 2014 17:27:31

[7]S. I. Woods, S. Ingvarsson, J. R. Kirtley, H. F. Hamann, and R. H. Koch, Appl. Phys. Lett. **81**, 1267 (2002).
[8]T. Veres, M. Cai, R. W. Cochrane, and S. Roorda, J. Appl. Phys. **87**, 8504 (2000).
[9]T. Veres, M. Cai, S. Germain, M. Rouabhi, F. Schiettekatte, S. Roorda, and R. W. Cochrane, J. Appl. Phys. **87**, 8513 (2000).
[10]S. Gangopadhyay, J. X. Shen, M. T. Kief, J. A. Barnard, and M. R. Parker, IEEE Trans. Magn. **31**, 3933 (1995).
[11]S.-H Ge, Y.-Y. Lü, Z.-Z. Zhang, C.-X. Li, T. Xu, and J.-Z. Zhao, J. Magn. Magn. Mater. **168**, 35 (1997).
[12]S. R. Teixeira *et al.*, J. Phys.: Condens. Matter **6**, 5545 (1994).
[13]P. Auric, S. R. Teixeira, B. Dieny, A. Chamberod, and O. Redon, J. Magn. Magn. Mater. **146**, 153 (1995).
[14]S. van Dijken, X. Jiang, and S. S. P. Parkin, Appl. Phys. Lett. **82**, 775 (2003).
[15]J. P. Biersack and L. G. Haggmark, Nucl. Instrum. Methods **174**, 257 (1980).
[16]H. Tolentino, D. Z. Cruz, V. Compagnon-Cailhol, E. Tamura, and M. C. Martins Alves, J. Synchrotron Radiat. **5**, 521 (1998).
[17]T. J. Ressler, J. Synchrotron Radiat. **5**, 118 (1998).
[18]B. K. Teo, *EXAFS: Basics Principles and Data Analysis*, 1st ed. (Springer, Germany, 1986), Chap. 6, p. 125.
[19]T. Devolder, Phys. Rev. B **62**, 5794 (2000).
[20]H. P. Klug and L. E. Alexander, *X-ray Diffraction Procedures*, 2nd ed. (Wiley, New York, 1974), Chap. 5, p. 290.
[21]B. Gilles, in *Thin Film Characterization by Advanced X-Ray Diffraction Techniques*, 1st ed., edited by G. Cappuccio (SIS Publications, Frascati, 1996), p. 177.
[22]A. R. Miedema, Philips Tech. Rev. **36**, 217 (1976).
[23]W. H. Flores, S. R. Teixeira, J. B. M. da Cunha, M. C. Martins Alves, H. Tolentino, and A. Traverse, Phys. Rev. B **61**, 3286 (2000).
[24]T. Nishizawa and K. Ishida, in *Binary Alloy Phase Diagrams*, 2nd ed., edited by T. B. Massalski (ASM International, Materials Park, 1996), Vol. 2, p. 1186.
[25]N. Mattoso, V. Fernandes, M. Abbate, W. H. Schreiner, and D. H. Mosca, Electrochem. Solid-State Lett. **4**, C20 (2001).

[This article is copyrighted as indicated in the article. Reuse of AIP content is subject to the terms at: http://scitation.aip.org/termsconditions. Downloaded to] IP: 200.130.19.173 On: Fri, 21 Mar 2014 17:27:31